

**Ab initio calculations for the interconversion of optically active defects in amorphous silica**M. M. G. Alemany<sup>1</sup> and James R. Chelikowsky<sup>2</sup><sup>1</sup>*Departamento de Física de la Materia Condensada, Facultad de Física, Universidad de Santiago de Compostela, E-15782 Santiago de Compostela, Spain*<sup>2</sup>*Center for Computational Materials, Institute for Computational Engineering and Sciences, Departments of Physics and Chemical Engineering, University of Texas, Austin, Texas 78712, USA*

(Received 13 July 2005; published 22 June 2006)

Using *ab initio* calculations on clusters, we have identified a new reaction path between the dicoordinated silicon atom defect and the paramagnetic  $E'_\gamma$  center in amorphous silica. Under ionizing irradiation, the dicoordinated silicon atom interacts with a nearby oxygen atom relaxing into a structure in which the unpaired electron is distributed between two threefold-coordinated silicon atoms. The transformation into the  $E'_\gamma$  center follows by a subsequent formation of a puckered configuration.

DOI: [10.1103/PhysRevB.73.235211](https://doi.org/10.1103/PhysRevB.73.235211)

PACS number(s): 61.72.Ji, 61.43.Fs, 68.35.Dv

Because of its unique mechanical, thermal, and optical characteristics, amorphous silicon dioxide ( $a\text{-SiO}_2$ ) is a material of great technological interest. As such, enormous interest has centered on understanding the structure and formation of point defects in  $a\text{-SiO}_2$ . Of special interest are defects that significantly affect the particular properties of ( $a\text{-SiO}_2$ )-based materials, e.g., defects that adversely affect properties or defects that can serve as a basis for new technologies such as photoinduced Bragg gratings. Belonging to such a class of defects are the diamagnetic oxygen deficiency centers ODC(I) and ODC(II) and the paramagnetic  $E'$  centers.<sup>1</sup> ODC(I) and ODC(II) give rise, respectively, to the photoabsorption bands at 7.6 and 5.0 eV. The family of  $E'$  centers comprises the paramagnetic centers characterized by a threefold-coordinated silicon atom with an unpaired electron,  $\equiv\text{Si}^\bullet$  (where  $\equiv$  and  $\bullet$  represent three Si—O bonds and the unpaired electron, respectively). The most important member of this defect family is the  $E'_\gamma$  center, which is defined by a strong <sup>29</sup>Si hyperfine interaction ( $A \sim 42$  mT) between the unpaired electron and the Si atom on which it is primarily located.

The atomic models for these centers not only have to address their electronic signatures, but also must address the fundamental interconversions known to occur between them. ODC(I) is identified as the “relaxed oxygen vacancy,”  $\equiv\text{Si}-\text{Si}\equiv$ . This structure is obtained by relaxation of the defect that arises by removal of the oxygen linking two vertex-sharing  $\text{SiO}_4$  tetrahedra,  $\equiv\text{Si}-\text{O}-\text{Si}\equiv$ , which is the unit predominantly determining short-range order in  $a\text{-SiO}_2$ . The model widely accepted for ODC(II) is the “dicoordinated silicon” or “divalent defect,” i.e., a silicon atom bonded to two oxygens and with a lone pair of electrons,  $=\text{Si}^\bullet$ . Based on these models, theory is able to explain both the 7.6 and 5.0 eV silica absorption bands,<sup>2,3</sup> as well as the experimentally proposed ODC(I)-to-ODC(II) interconversion in the neutral excited state.<sup>4</sup> Experiment also indicates that both diamagnetic centers transform into the  $E'_\gamma$  center upon exposure to ionizing irradiation.<sup>5,6</sup> The ODC(I)  $\rightarrow$   $E'_\gamma$  center transformation has been widely studied and is generally accepted as a model for the formation of  $E'_\gamma$  centers in  $a\text{-SiO}_2$ . According to this model, the ionization of the oxygen vacancy results in the puckered configuration  $\equiv\text{Si}^+$

$\equiv\text{Si}^+-\text{O}=\equiv$ , in which the silicon atom carrying the trapped hole,  $+$ , interacts with an additional neighboring oxygen atom located behind those to which it is initially bonded (in case there is no such oxygen atom at a particular defect site, the hole captured at the oxygen vacancy is released until captured at a puckered-precursor site<sup>7</sup>). This model for the  $E'_\gamma$  center follows the model of Rudra and Fowler for the  $E'_1$  defect in  $\alpha$ -quartz<sup>8</sup> (its crystalline counterpart), and it was first adopted by Boero *et al.*<sup>9</sup> (extensive studies on this model transformation as a function of the oxygen vacancy site in the amorphous network have been recently reported<sup>7,10</sup>). An alternative model for the  $E'_\gamma$  center,  $=(\text{Si}^\bullet)-\text{O}-(\text{Si}^+) =$ , not involving ODC(I) as a precursor but a neutral edge-sharing pair of  $\text{SiO}_4$  tetrahedra which has lost one of its bridging oxygen atoms, has been recently proposed by Uchino, Takahashi, and Yoko.<sup>11</sup> Theoretical evidence for the existence of such a pair in  $a\text{-SiO}_2$  has been obtained through molecular-dynamics simulations based on a *model* potential<sup>12</sup> and *ab initio* calculations.<sup>13</sup>

The ODC(II)  $\rightarrow$   $E'_\gamma$  center interconversion within the divalent defect model has been less understood. Only recently a model for this interconversion has been put forward by Donadio, Bernasconi, and Boero.<sup>4</sup> According to this model, the dicoordinated silicon, upon removal of one of its unpaired electrons, interacts with a nearby oxygen atom yielding two separate units, one unit including the  $E'_\gamma$  center,  $\equiv\text{Si}-\text{O}-\text{Si}^\bullet =$ , the other unit holding the positive charge,  $\equiv\text{Si}^+$ . In this model, the latter unit is stabilized by forming from its silicon atom a bond with an additional oxygen atom from the amorphous network. Here we will show that the stabilization of this unit can also be done via electrostatic interaction with the silicon atom holding the unpaired electron in the  $\equiv\text{Si}-\text{O}-\text{Si}^\bullet =$  unit. In this case, as we will see, a new reaction path between the divalent defect and the  $E'_\gamma$  center in  $a\text{-SiO}_2$  can be determined. The reaction path identified in this work involves the formation of a puckered configuration, similarly to the well known ODC(I)<sup>+</sup>-to- $E'_\gamma$  interconversion.

We performed our calculations within a real-space pseudopotential approach<sup>14</sup> based on Kohn-Sham density-functional theory.<sup>15</sup> We place the cluster of interest at the center of a spherical domain chosen so the wave functions

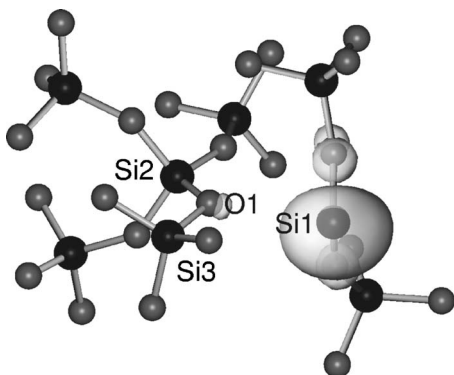


FIG. 1. The  $\text{Si}_8\text{O}_{24}\text{H}_{18}$  cluster modeling the divalent defect in amorphous silica after full geometrical optimization. Hydrogen atoms (not shown) were used to saturate the dangling bonds of the outer oxygen atoms. The electron-density surfaces correspond to the lone pair of electrons of the divalency mainly localized on the dicoordinated silicon atom, Si1.

smoothly vanish at its boundary. Hydrogen atoms were used to saturate the dangling bonds of the outer (oxygen) atoms. The core electrons were represented by norm-conserving pseudopotentials using the Troullier-Martins prescription.<sup>16</sup> The local spin density approximation given by Ceperley and Alder was used for the exchange and correlation potential.<sup>17</sup>

Real-space techniques permit systematic studies of convergence in the spirit of plane-wave methods since only one parameter, the grid spacing, need be refined. This contrasts with methods that employ local orbitals as basis, which require extensive testing of the basis by optimizing a multiple-parameter space, and can yield results sensitive to the basis choice. Also, charge states are easily handled in a natural manner in real-space approaches, i.e., unlike supercell methods, no compensating background charge need be invoked. Local minima structures were sought using a uniform grid with a grid spacing of  $h=0.35$  a.u. [or an equivalent plane-wave cutoff of  $\sim(\pi/h)^2 \sim 80$  Ry]. The structures were further optimized with a final grid spacing of 0.30 a.u. ( $\sim 120$  Ry). All the atoms in the cluster, including the terminating hydrogen atoms, were allowed to relax, otherwise stated. (The same computational method employed here was used in our previous work on the characterization of the  $E'_\gamma$  center model of Uchino, Takahashi, and Yoko.<sup>13</sup>)

In Fig. 1, we plot the structure used for modeling the divalent defect in  $a\text{-SiO}_2$ . This structure was constructed from a model configuration of the divalent defect obtained from an *ab initio* molecular-dynamics simulation of  $a\text{-SiO}_2$ . In this simulation, an oxygen was removed from the sample during a high-temperature regime, and the sample cooled down to ambient temperature without imposing any constraints. (The stabilization and quenching procedure employed for sampling of the phase space were the same as that used in our previous work.<sup>13</sup>) We find the structural parameters characterizing the divalent defect in good agreement with previous theoretical results. The dicoordinated silicon, Si1, forms bonds of 1.65 and 1.64 Å with both oxygen atoms, and an angle of 101.0°, similar to values reported previously, 1.64–1.68 Å and 98°–101°,<sup>1</sup> respectively. The next closest oxygen atom to Si1 is O1 at a distance of 2.71 Å.

Silicon atoms other than Si1 form Si—O bonds of  $1.62 \pm 0.01$  Å, in excellent agreement with the experimental value obtained for  $a\text{-SiO}_2$  in the neutral state, 1.62 Å.<sup>18</sup>

In order to simulate the ionization process, we remove one electron from our divalent defect model and look for local minima configurations by optimizing the geometry. We find that two different relaxation paths are possible depending on the way Si1 moves with respect to the silicon atoms that O1 bridges, Si2 and Si3. A “symmetric” relaxation yields the structure illustrated in Fig. 2(a). The main effects of the ionization process are the excitation of one of the lone pair of electrons on Si1 to the conduction band, and a reduction of the distance between Si1 and O1 (by 0.82 Å) owing to the residual positive charge localized mainly on Si1. Si1, which becomes threefold-coordinated, retains the unpaired electron in an  $sp^3$ -like dangling bond, as indicated by the average of the O-Si1-O angles, 109.6°. However, the calculated value for the isotropic hyperfine interaction  $A$  between the unpaired electron and the  $^{29}\text{Si}$  nucleus of Si1 precludes  $\equiv\text{Si1}^*$  for being part of the  $E'_\gamma$  center in  $a\text{-SiO}_2$ . Using the Van de Walle and Blöchl prescription for calculating the hyperfine interaction,<sup>19</sup> we obtained a value for  $A$  of 64.0 mT, which is significantly higher than the value extracted from experiment,  $A \sim 42$  mT.

The divalent defect can also experience an “asymmetric” relaxation upon ionization. In Fig. 2(b), we present a model configuration for  $\text{ODC(II)}^+$  which is obtained by simultaneously breaking and forming an Si—O bond in the divalent model represented in Fig. 1 (Si2-O1 and Si1-O1 bonds, respectively). Besides the absence of a bond between Si2 and O1, this model configuration for  $\text{ODC(II)}^+$  differs from that represented in Fig. 2(a) by the formation of a stronger Si1-O1 bond (the bond is shortened by 0.29 Å). The hyperfine constant calculated at Si1 in the cluster model represented in Fig. 2(b) is 50.0 mT, which is in better agreement with the experimental value characteristic of the  $E'_\gamma$  center. However, we find this  $E'$ -center model to be highly unstable owing to the significant accumulation of positive charge in Si2. Slight perturbations on the local structure around Si2 drive relaxations into two different local minima configurations. One is the model cluster represented in Fig. 2(a), the relaxation driven by the Coulomb attraction between Si2 and O1. The other one is the local minimum structure represented in Fig. 2(c), Si2 attracting in this case Si1, the latter atom relaxing through the plane formed by the three oxygen atoms to which it is bonded. Local minima represented in Figs. 2(a) and 2(c) are degenerate (total energies differ only by 0.004 eV/at).

In the structure model represented in Fig. 2(c), the threefold-coordinated Si1 and Si2 atoms are 2.50 Å apart from each other forming a dimerlike configuration, with the unpaired electron being extended among them. This structural and electronic configuration resembles  $\text{ODC(I)}^+$ , i.e., what is believed to be a precursor of the  $E'_\gamma$  center in  $a\text{-SiO}_2$ .  $\text{ODC(I)}^+$  is also considered as a model for a second paramagnetic active center in  $a\text{-SiO}_2$ , the  $E'_\delta$  center, which is responsible for the hyperfine spectrum at 10 mT.<sup>7,10,20</sup> Calculation of the hyperfine constant at Si1 and Si2 gives an average value for this magnitude that agrees well with ex-

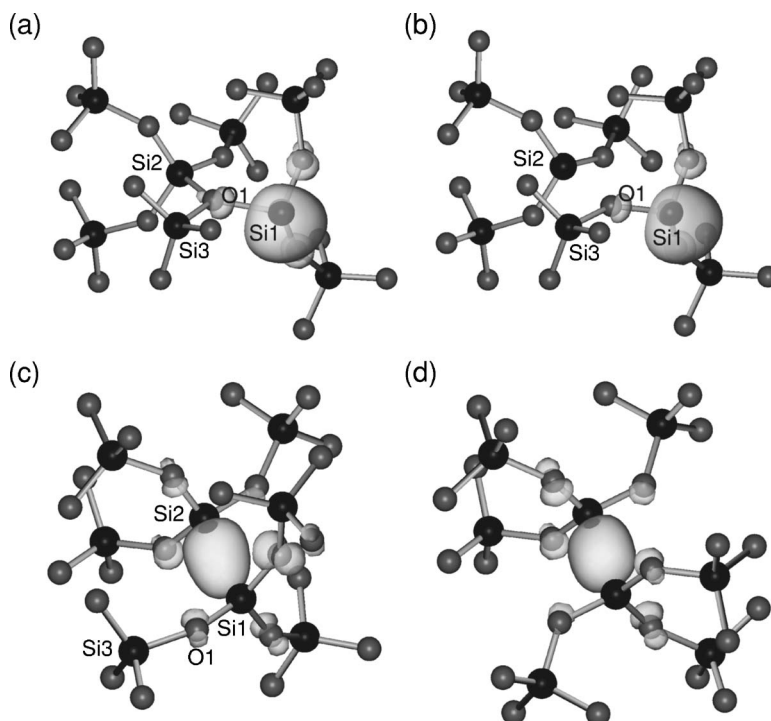


FIG. 2.  $(\text{Si}_8\text{O}_{24}\text{H}_{18})^+$  clusters, after optimization, describing the “symmetric” and “asymmetric” relaxation paths followed by the divalent defect model represented in Fig. 1 upon ionization (see the text). The electron-density surfaces correspond to the spin densities of the clusters, that is, to the difference between the charge densities of the spin-up and the spin-down electrons. (a) Final structure obtained from the “symmetric” relaxation. The structure reflects the Coulomb interaction between Si1 and O1 in Fig. 1 when the cluster is ionized. (b) Intermediate created structure during the “asymmetric” relaxation. The structure is obtained by forming a bond between Si1 and O1 in Fig. 1, while simultaneously breaking the Si2-O1 bond. The separation between Si2 and O1 in this structure was fixed to 2.50 Å. (c) Final structure obtained from the “asymmetric” relaxation. The formation mechanism of the structure is the electrostatic interaction between Si1 and Si2 in (b). (d) Model structure for the  $E'_\delta$  center in amorphous silica. The structure was constructed from the model cluster in (c) replacing the  $(\text{Si}_4\text{O}_{12}\text{H}_9)$  unit surrounding Si1 by one obtained inverting the  $(\text{Si}_4\text{O}_{12}\text{H}_9)$  unit surrounding Si2. Note the different distribution of the unpaired electron among the adjoining silicon atoms in the model clusters of (c) and (d). The electron does not distribute equally with respect to the silicon atoms in the former while it does in the latter.

periment, 11.4 mT, but this value differs notably from one silicon site to the other (4.7 and 18.1 mT, respectively). The origin of this “asymmetry” is in the Coulomb attraction exerted by Si2 in the transformation from the cluster model represented in Fig. 2(b) to that of Fig. 2(c), in which Si2 takes much of the unpaired electron. Also, this transformation results in a different accumulation of positive charge at both sites, being more important at Si2, as indicated by the average value of the Si1-O and Si2-O bonds, 1.59 and 1.57 Å, respectively.

From the distorted dimerlike configuration represented in Fig. 2(c), we constructed a model structure for  $\text{ODC}(\text{I})^+$  by inverting the  $\text{Si}_4\text{O}_{12}\text{H}_9$  cluster surrounding Si2 with respect to a point belonging to the line defined by Si2 and the barycenter of the triangle formed by its three O neighbors [Fig. 2(d)]. We find this constrained dimerlike structure to be energetically competitive with respect to the distorted one of Fig. 2(c), and also to be a good model for the  $E'_\delta$  center, as indicated by the value obtained for the hyperfine constant at both silicon sites, 12.0 mT. Thus, a transition from the distorted dimerlike structure to the undistorted one would be feasible in principle, although likely nontrivial since it would involve rearrangements of first- and second-neighbor  $\text{SiO}_4$  units surrounding the defect. We have performed molecular-

dynamics simulations by coupling the distorted dimer configuration of Fig. 2(c) to a heat bath at 300 K via the Langevin equation of motion,<sup>21</sup> which confirmed our assumption.

As we mentioned previously, the transformation from the  $\text{ODC}(\text{I})^+$  defect into a stable  $E'_\gamma$  center is believed to occur via the formation of a puckered configuration, i.e., by the formation of a new bond between one of the adjoining silicon atoms and an oxygen atom located behind the plane determined by its three oxygen neighbors.<sup>1</sup> In order to check the viability of this transformation within the distorted dimerlike model represented in Fig. 2(c), we added a water molecule to the cluster that would activate the process on each of the silicon sites. The molecule was located in such a way that its oxygen atom (O2) was placed in the direction determined by the silicon atom (Si1 or Si2) and the barycenter of the triangle formed by the three oxygen atoms to which it is bonded, 2.5 Å separated from the silicon atom. Each cluster was then relaxed by moving their constituent atoms (but the hydrogens of the water molecule were kept at their initial positions) in the direction of the forces acting on them. Owing to the “asymmetry” of the dimerlike cluster, and in particular to the different amount of positive charge accumulated at Si1 and Si2, the results obtained from both structural optimizations were different. When the water mol-



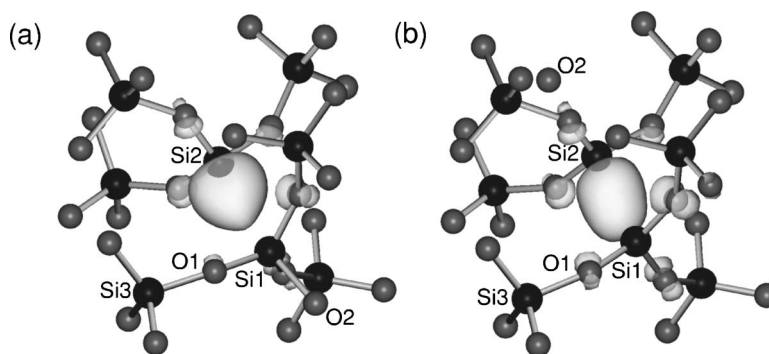


FIG. 3.  $(\text{Si}_8\text{O}_{25}\text{H}_{20})^+$  clusters, after optimization, obtained from the model cluster of Fig. 2(c) by adding a water molecule (with oxygen atom labeled O2) to the cluster. The water molecule was placed behind the  $\text{Si1O}_3$  and  $\text{Si2O}_3$  units in (a) and (b), respectively. The hydrogen atoms used for saturating the outermost oxygen atoms are not shown. The electron-density surfaces correspond to the spin densities of the clusters. In (a), a model cluster for the  $\text{E}'_\gamma$  center in amorphous silica is obtained via formation of a puckered configuration. (b) corresponds to a distorted dimerlike structure similar to that represented in Fig. 2(c). The hydrogen atoms of the water molecule were kept at their initial positions during the optimization.

ecule is placed on the Si1 side, only one local minimum is obtained. This minimum corresponds to the formation of an  $\text{E}'_\gamma$  center [Fig. 3(a)]. During the minimization, Si1 puckers through the plane formed by the three oxygen atoms to which it is initially joined following the electrostatic interaction with O2. The unpaired electron resides in an  $sp^3$ -like dangling bond of Si2. Calculation of the hyperfine constant at Si2 gives a value of 44.5 mT, in very good agreement with the value characteristic for the  $\text{E}'_\gamma$  center,  $\sim 42$  mT. In contrast, when O2 is placed behind the  $\text{Si2O}_3$  unit in Fig. 2(c), a dimerlike local minimum configuration that does not involve puckering is obtained [Fig. 3(b)]. We find the total energy of the latter configuration to be 0.022 eV/at higher than that of the  $\text{E}'_\gamma$  center model of Fig. 3(a), which indicates that puckering is favored within our distorted dimerlike model.

Thus, the reaction path we propose between the divalent defect model and the paramagnetic  $\text{E}'_\gamma$  center entails three steps that can be represented as  $(\text{Fig. 1})^+ \rightarrow \text{Fig. 2(b)} \rightarrow \text{Fig. 2(c)} \rightarrow \text{Fig. 3(a)}$ . The first two steps only involve the interaction between nearest neighbors atoms expected to surround the divalent defect (Si2 and O1, as part of the same tetrahedra  $\text{SiO}_4$  unit), and the atoms that constitute the divalent defect itself (Si1). The last step is accomplished by the formation of a puckered configuration, similarly to the fundamental  $\text{ODC(I)}^+ \rightarrow \text{E}'_\gamma$  interconversion. As mentioned in the Introduction, Donadio, Bernasconi, and Boero have recently proposed a reaction path between the dicoordinated silicon and the  $\text{E}'_\gamma$  center.<sup>4</sup> Their proposed path can be defined via the stabilization of the transient structure plotted in Fig. 2(b) by formation of an Si-O bond between Si2 and an additional oxygen atom from the amorphous network. Such stabilization will not disturb the structural and electronic properties of the cluster in the surroundings of Si1, thus explaining the characterization features of the  $\text{E}'_\gamma$  center. The reaction path they proposed was determined to be nearly barrierless by performing *ab initio* simulations on a periodic model of  $a\text{-SiO}_2$ .

In order to estimate the energy cost of the  $\text{ODC(II)} \rightarrow \text{E}'_\gamma$  center interconversion proposed in this work, we have repeated the first two steps of the interconversion while

keeping fixed the hydrogen atoms at the boundary. This allows us to obtain an upper limit value for the energy barrier, since the relaxation energy of the amorphous network surrounding the transforming process is clearly underestimated. We first brought the divalent defect model of Fig. 1 into the transient structure of Fig. 2(b) through a series of intermediate configurations in which all the degrees of freedom, save the positions of the atoms labeled as Si1, Si2, Si3, and O1 (besides the hydrogen atoms), were allowed to relax. (The Si1, Si2, Si3, and O1 atoms determine the reaction path between the two structures.) The energy penalty of this process was calculated to be as low as 0.4 eV. The transient structure was then brought to the distorted  $\text{E}'_\delta$  center [Fig. 2(c)] by simply controlling the distance between Si1 and Si2. This latter process was found to have no energy cost. Thus, the activation barrier of the interconversion we propose in this work takes some value between zero and 0.4 eV.

In summary, we have identified a reaction path for the formation of  $\text{E}'_\gamma$  centers from divalent defects in irradiated  $a\text{-SiO}_2$ . The importance of our finding not only resides in the identification of a new creation mechanism for the fundamental  $\text{E}'_\gamma$  paramagnetic center in  $a\text{-SiO}_2$ , it also reinforces the divalent defect as an atomic model for  $\text{ODC(II)}$  capable of explaining both the properties characteristic of this center and the experimentally observed microscopic processes to which it is related.

This work was funded in part by the National Science Foundation under Grants No. DMR-0130395 and No. DMR-0325218 and the U.S. Department of Energy under Contracts No. DE-FG02-89ER45391 and No. DE-FG02-03ER15491. Computational support was provided by the National Energy Research Scientific Computing Center, the Minnesota Supercomputer Institute, and the Galician Supercomputer Center (CESGA). M.M.G.A. acknowledges support from the Spanish Ministry of Education and Science (Program “Ramón y Cajal”) and the Spanish Ministry of Education and Science in conjunction with the European Regional Development Fund (Project FIS2005-04239).

- <sup>1</sup>For a review, see, for example, L. Skuja, *J. Non-Cryst. Solids* **239**, 16 (1998).
- <sup>2</sup>G. Pacchioni and G. Ieranò, *Phys. Rev. Lett.* **79**, 753 (1997).
- <sup>3</sup>B. L. Zhang and K. Raghavachari, *Phys. Rev. B* **55**, R15993 (1997).
- <sup>4</sup>D. Donadio, M. Bernasconi, and M. Boero, *Phys. Rev. Lett.* **87**, 195504 (2001).
- <sup>5</sup>H. Imai, K. Arai, H. Imagawa, H. Hosono, and Y. Abe, *Phys. Rev. B* **38**, 12772 (1988).
- <sup>6</sup>H. Imai, K. Arai, H. Hosono, Y. Abe, T. Arai, and H. Imagawa, *Phys. Rev. B* **44**, 4812 (1991).
- <sup>7</sup>Z.-Y. Lu, C. J. Nicklaw, D. M. Fleetwood, R. D. Schrimpf, and S. T. Pantelides, *Phys. Rev. Lett.* **89**, 285505 (2002).
- <sup>8</sup>J. K. Rudra and W. B. Fowler, *Phys. Rev. B* **35**, 8223 (1987).
- <sup>9</sup>M. Boero, A. Pasquarello, J. Sarnthein, and R. Car, *Phys. Rev. Lett.* **78**, 887 (1997).
- <sup>10</sup>S. Mukhopadhyay, P. V. Sushko, A. M. Stoneham, and A. L. Shluger, *Phys. Rev. B* **70**, 195203 (2004).
- <sup>11</sup>T. Uchino, M. Takahashi, and T. Yoko, *Phys. Rev. Lett.* **86**, 5522 (2001).
- <sup>12</sup>K. Vollmayr, W. Kob, and K. Binder, *Phys. Rev. B* **54**, 15808 (1996).
- <sup>13</sup>M. M. G. Alemany and J. R. Chelikowsky, *Phys. Rev. B* **68**, 054206 (2003).
- <sup>14</sup>J. R. Chelikowsky, N. Troullier, and Y. Saad, *Phys. Rev. Lett.* **72**, 1240 (1994).
- <sup>15</sup>P. Hohenberg and W. Kohn, *Phys. Rev.* **136**, B864 (1964); W. Kohn and L. J. Sham, *Phys. Rev.* **140**, A1133 (1965).
- <sup>16</sup>N. Troullier and J. L. Martins, *Phys. Rev. B* **43**, 1993 (1991).
- <sup>17</sup>D. M. Ceperley and B. J. Alder, *Phys. Rev. Lett.* **45**, 566 (1980).
- <sup>18</sup>R. L. Mozzi and B. E. Warren, *J. Appl. Crystallogr.* **2**, 164 (1969).
- <sup>19</sup>C. G. Van de Walle and P. E. Blöchl, *Phys. Rev. B* **47**, 4244 (1993).
- <sup>20</sup>J. R. Chavez, S. P. Karna, K. Vanheusden, C. P. Brothers, R. D. Pugh, B. K. Singaraju, W. L. Warren, and R. A. B. Devine, *IEEE Trans. Nucl. Sci.* **44**, 1799 (1997).
- <sup>21</sup>N. Binggeli, J. L. Martins, and J. R. Chelikowsky, *Phys. Rev. Lett.* **68**, 2956 (1992).